



Supplement of

Sensitivity of a Sahelian groundwater-based agroforestry system to tree density and water availability using the land surface model ORCHIDEE (r7949)

Espoir Koudjo Gaglo et al.

Correspondence to: Espoir Koudjo Gaglo (espoirkoudjo.gaglo@ucad.edu.sn)

The copyright of individual parts of the supplement might differ from the article licence.

Supplementary material

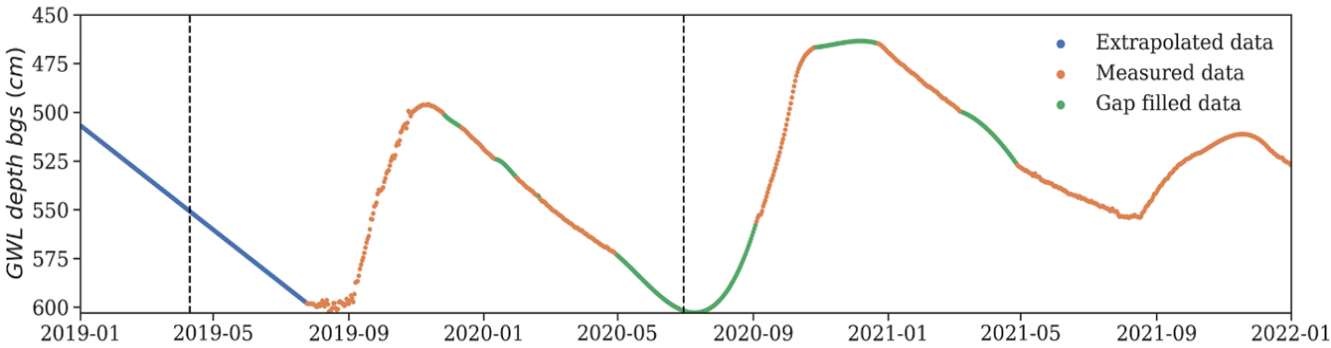


Figure S1: Groundwater dynamic (GWL) and depth below the ground surface (bgs). Source: Diongue et al., (2023).

5

10

15

20

25

30

35

Table S1: List of parameters used in ORCHIDEE for millet and *Faidherbia albida*

| Process involved and parameters descriptions | Parameters notations | Values | | References | |
|--|-------------------------|---------|------|---|------|
| | | Tree | Crop | Tree | Crop |
| Soil properties | | | | | |
| Clay fraction (%) | clay_fraction | 4 | | Diongue et al., (2022) Roupsard et al., (2020) | |
| Silt fraction (%) | silt_fraction | 12.45 | | | |
| Sand fraction (%) | sand_fraction | 87.15 | | | |
| Bulk density (kg m ⁻³) | bulk_default | 1710 | | | |
| Soil pH (-) | soil_ph | 5.75 | | | |
| Flag to prescribe soil type (-) | impose_soilt | TRUE | | This study | |
| Soil depth | | | | | |
| Maximum depth of soil moisture (m) | depth_max_h | 7 | | Siegwart et al., (2023) | |
| Maximum depth of the root profile (m) | max_root_depth | 7 | 2 | | |
| Maximum active layer thickness (m) | maxaltmax | 15 | | This study | |
| Start depth of constant layer thickness (m) | depth_cstthick | 0.123 | | This study | |
| Soil water content forcing | | | | | |
| Depth at which the hydrology layers will be refined towards the bottom (-) | refinebottom | TRUE | | This study | |
| Activate nudging of soil moisture (-) | ok_nudge_mc | TRUE | | | |
| Prescribed water depth (m) | zwt_force | 4 | 10 | | |
| Soil hydraulic | | | | | |
| Retention curve coefficient (n) (-) | nvan_imp | 1.89 | | Diongue et al., (2022) | |
| Retention curve coefficient (α) (m m ⁻¹) | avan_imp | 0.00075 | | | |
| Residual water content (m ³ m ⁻³) | mcr_imp | 0.065 | | | |
| Saturated water content (m ³ m ⁻³) | mcs_imp | 0.43 | | | |
| Hydraulic conductivity saturation (mm d ⁻¹) | ks_imp | 1060 | | | |
| Water content at field capacity (m ³ m ⁻³) | mcfc_imp | 0.11 | | | |
| Water content at wilting point (m ³ m ⁻³) | mcw_imp | 0.0884 | | | |
| Activation flag Van Genuchten model (-) | is_vg | TRUE | | This study | |
| Soil conductivity decay factor (-) | kfact_decay_rate | 0 | | This study | |
| Development and phenological stages | | | | | |
| Minimum time since season (days) | min_growthinit_time | 315 | 340 | This study | |
| Minimum time elapsed | hum_min_time | 360 | 350 | | |
| Leaf longevity (days) | longevity_leaf | 170 | 200 | | |
| Length of leaf senescence (days) | leaffall | 30 | 20 | | |
| Timescales for phenology process (days) | tau_hum_month | 25 | | | |
| Monthly temperature threshold above which tendency doesn't matter (°C) | t_always_add | 11 | | | |

45 **Table S1. (continued)**

| Process involved and parameters descriptions | Parameters notations | Values | | References | |
|---|-------------------------|--------|-------|--------------------------|-----------------------|
| | | Tree | Crop | Tree | Crop |
| Leaf area index | | | | | |
| Minimum leaf-to-sapwood area ratio (-) | k_latosa_min | 5000 | 6000 | This study | |
| Maximum leaf-to-sapwood area ratio (-) | k_latosa_max | 6000 | 7000 | | |
| Allometric | | | | | |
| Wood density (gC m ⁻³) | pipe_density | 280250 | - | Wickens, (1995) | - |
| Form factor for cylinder volume reduction (-) | tree_ff | 0.6 | - | This study | - |
| Height factor (-) | pipe_tune3 | 0.25 | - | This study | - |
| Height factor (-) | pipe_tune2 | 15 | - | This study | - |
| Minimum diameter of a new stand (m) | dia_init_min | 0.01 | - | This study | - |
| Maximum diameter of a new stand (m) | dia_init_max | 0.02 | - | This study | - |
| Height of a new vegetation (m) | height_init | - | 0.1 | - | This study |
| Conversion factor from LAI to height (-) | lai_to_height | - | 0.6 | - | This study |
| Total of plants (ind ha ⁻¹) | nmaxplants | - | 9000 | - | Sow et al., (2024) |
| Canopy cover (-) | canopy_cover | - | 0.81 | - | Sow et al., (2024) |
| Photosynthesis and carbon allocation | | | | | |
| Lower bound factor for nitrogen use efficiency (-) | sugar_load_min | 0.9 | | This study | This study |
| Light absorption efficiency (mol e [−] (mol photon) ^{−1}) | alpha_LL | 1 | 0.5 | This study | This study |
| Intercept of Jmax25/Vcmax25 (μmol e [−] (μmol CO ₂) ^{−1}) | arJV | 1.95 | 2 | This study | This study |
| Slope of Jmax25/Vcmax25 (μmol e [−] (μmol CO ₂) ^{−1}) | brJV | 0 | 0 | This study | This study |
| Nitrogen use efficiency (μmol [CO ₂] s ^{−1}) (gN[leaf]) ^{−1}) | nue_opt | 120 | 60 | This study | Kattge et al., (2009) |
| Deactivation energy for Vcmax (kJ mol ^{−1}) | D_Vcmax | 202.9 | 192 | Harley et al., (1992) | Massad et al., (2007) |
| Deactivation energy for Jmax (kJ mol ^{−1}) | D_Jmax | 201 | 192 | Harley et al., (1992) | Massad et al., (2007) |
| Entropy term function for Vcmax (J K ^{−1} mol ^{−1}) | aSV | 650 | 641.6 | Harley et al., (1992) | Default |
| Convexity term for electron transport (-) | theta | 0.9 | 0.7 | Thornley, (2002) | Von Caemmerer, (2000) |
| Activation energy for Vcmax (kJ mol ^{−1}) | E_Vcmax | 65.33 | 67.30 | Chen et al., (2008) | This study |
| Activation energy for Jmax (kJ mol ^{−1}) | E_Jmax | 79.5 | 77.9 | Chen et al., (2008) | Massad et al., (2007) |
| Entropy term function for Jmax (J K ^{−1} mol ^{−1}) | aSJ | 650 | 630 | Chen et al., (2008) | Massad et al., (2007) |
| Michaelis–Menten constant for O ₂ at 25°C (mbar) | kmO25 | 414.5 | 450 | Chen et al., (2008) | Von Caemmerer, (2000) |
| Michaelis–Menten constant for CO ₂ at 25°C (μbar) | kmC25 | 270 | 650 | Bernacchi et al., (2002) | Von Caemmerer, (2000) |
| Rubisco specificity factor (bar bar ^{−1}) | Sco25 | 2321 | 2590 | Harley et al., (1992) | Von Caemmerer, (2000) |
| Evapotranspiration and vegetation structure | | | | | |
| Structural resistance (s m ^{−1}) | rstruct_const | 2 | 0.002 | This study | |
| Canopy resistance parameter (-) | rveg_pft | 0.01 | 0.7 | | |
| Structural resistance (s m ^{−1}) | rstruct_const | 2 | 0.002 | | |

Table S2: Plant functional types (PFT) and their fraction used in this study.

| Plant functional type | 0 trees | 7 trees | 13 trees | 26 trees |
|---------------------------------------|---------|---------|----------|----------|
| Bare soil | 0.1 | 0.1 | 0.1 | 0.1 |
| Tropical deciduous summer-green trees | 0 | 0.075 | 0.15 | 0.3 |
| C4 crop | 0.9 | 0.825 | 0.75 | 0.6 |

50

55

60

65

70

75

80

85

90 S1. Vegetation water stress calculation

In the ORCHIDEE model, vegetation's water stress is used to trigger phenology and influence vegetation growth. Vegetation's water stress for *Faidherbia albida* is calculated across the entire soil column, incorporating the functional root profile as a weighting factor. The root profile, representing the fraction of root mass distributed across each soil layer based on the availability of water, is defined as:

$$95 \quad Rf(i) = \begin{cases} 0, & \text{if } i < i_{4m} \\ 0, & \text{if } i \geq i_{4m} \text{ and } \sum_{i=i_{4m}}^n \max(0, W_i - W_{p,i}) \leq 0 \\ \frac{\max(0, W_i - W_{p,i})}{\sum_{i=i_{4m}}^n \max(0, W_i - W_{p,i})}, & \text{if } i \geq i_{4m} \text{ and } \sum_{i=i_{4m}}^n \max(0, W_i - W_{p,i}) > 0 \end{cases} \quad (S1)$$

where i is the index for each soil layer, i_{4m} represents the index of the soil layer at 4 m, Rf represents the root profile at position i (unitless) and ranges between 0 and 1, n is the total of soil layers, W_i represents the soil moisture at position i (kg m^{-2}) and $W_{p,i}$ represents the wilting point moisture at position i (kg m^{-2}).

Then, vegetation water stress (W_{stress}) for *Faidherbia albida* is then given by:

$$100 \quad W_{\text{stress}} = \sum_{i=1}^n \min \left(1, \max \left(0, \frac{(W_i - W_{p,i})}{(W_{f,i} - W_{p,i})} \right) \right) \times Rf(i) \quad (S2)$$

where i is the index for each soil layer, n is the total of soil layers, W_i represents the soil moisture at position i (kg m^{-2}), $W_{p,i}$ represents the wilting point moisture at position i (kg m^{-2}) and $W_{f,i}$ is the soil moisture of each layer at field capacity (kg m^{-2}).

105

110

115

120

S2. In-situ climate data description

125 Mean annual air temperature was 27.78°C, with extremes' daily means ranging from a minimum of 20.27°C in 2021
to a maximum of 34.91°C in 2023. The data revealed interannual variability in precipitation, where 2022 was the
wettest year (821.62 mm of cumulative annual rain) while 2018 and 2021 were drier (454.42 mm and 482.37 mm of
cumulative annual rain). The years 2019, 2020, and 2023 experienced moderate rainfall, with totals of 513 mm, 599
mm, and 537 mm of cumulative annual rain, respectively. Relative humidity fluctuated between extremes' daily of
130 6.09% and 94.60%, observed in 2018 and 2022 respectively, with a yearly mean of 53.90%. Daily atmospheric
pressure varied from 1002.03 hPa in 2022 to 1012.96 hPa in 2018, with a yearly mean of 1006.96 hPa. Daily wind
speeds ranged from 1.20 m s⁻¹ to 7.27 m s⁻¹ both recorded in 2023, with an annual mean wind speed of 3.23 m s⁻¹.
Shortwave radiation experienced a daily minimum of 67.80 W m⁻² in 2020 and a daily maximum of 383.20 W m⁻² in
2022, with a yearly mean of 283 W m⁻². Long-wave radiation measurements indicated a daily minimum of 323.40 W
135 m⁻² in 2023 and a daily maximum of 350.88 W m⁻² in 2021, with a yearly average of 337.34 W m⁻².

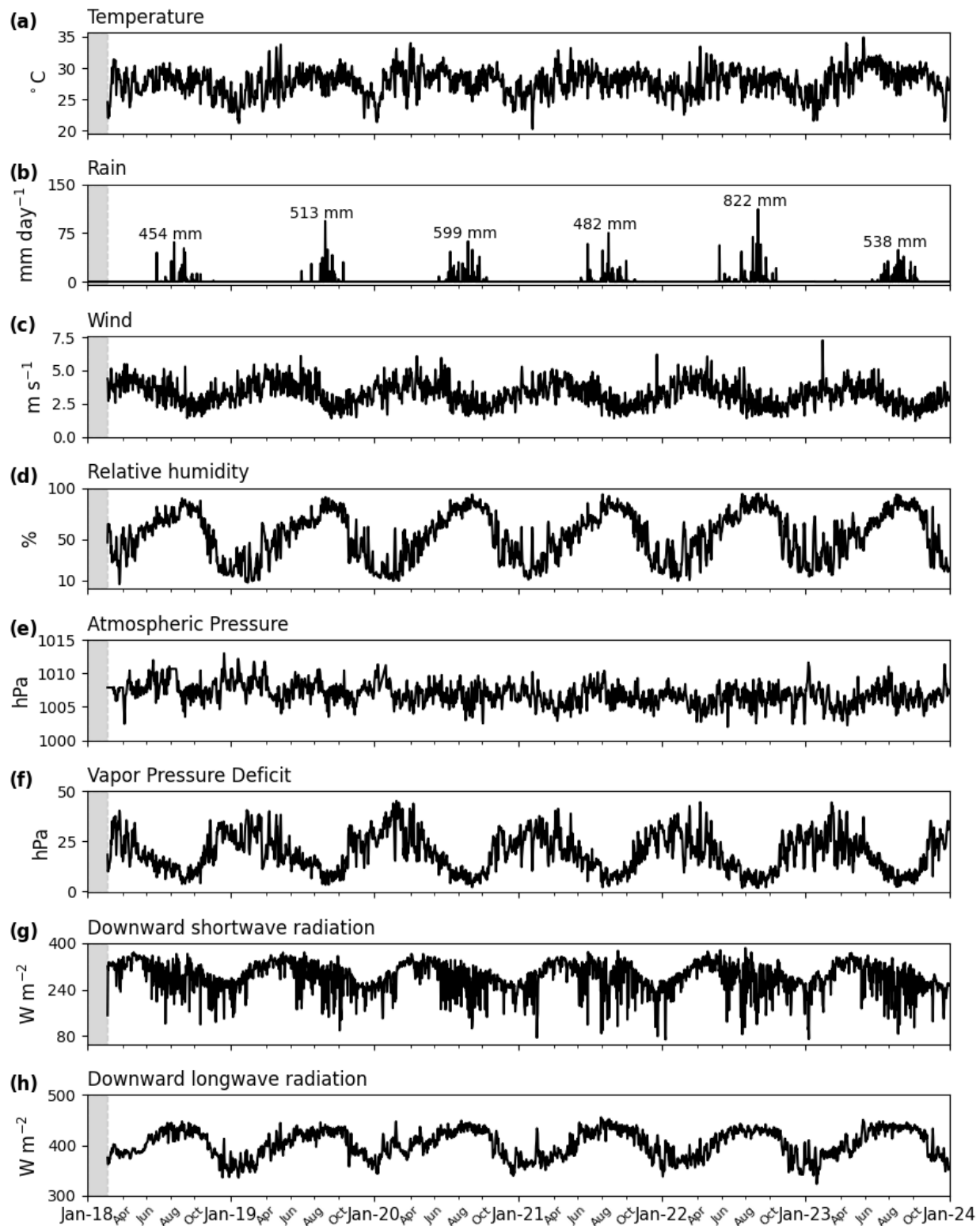


Figure S2: Daily time series of each in situ climate variable: (a) temperature, (b) rainfall and its cumulative annual rain, (c) wind, (d) relative humidity, (e) atmospheric pressure, (f) vapor pressure deficit, (g) downward longwave radiation, (h) downward shortwave radiation. The gray band represents the period of missing data.

S3. Average cycles of rainfall and soil water content in the capillary fringe

The average yearly cycles were calculated from total annual rainfall throughout five years, from 2018 to 2022 for precipitation, and from 2019 to 2021 for soil water content in the capillary fringe of the groundwater table (SWCC) with values as detailed below. For the average precipitation cycle, the average annual sum of precipitation over the analysis period was 574 mm. The maximum recorded rainfall in a single day was 81 mm. The average precipitation, calculated over the five years, was 1.59 ± 7.26 mm per day for 52 rainy days per year. The first rainy day, second rainy day, second-to-last rainy day, and last rainy day were recorded as 18 May, 20 June, 22 October, and 17 November, respectively. The second-to-last and the end of the rainy season were recorded as 22 October and 17 November, respectively. In addition, a daily average of temperature and relative humidity over the 5 years was used to constitute the average climate values for the various sensitivity analyses.

SWCC_{avg} was not calculated as a simple yearly average cycle, instead some key dates and amplitudes of the SWCC cycle and combined with linear interpolation in between those points resulting in the cycle shown in Fig. S3. Indeed, at the beginning of the year (1 January), SWCC averaged $0.26 \text{ m}^3 \text{ m}^{-3}$ and gradually declined to its minimum of $0.15 \text{ m}^3 \text{ m}^{-3}$ by 8 July, marking the driest period of the year. This low level persisted until 10 September, after which a rapid recharge phase began, reaching its peak value of $0.31 \text{ m}^3 \text{ m}^{-3}$ on 24 October. By 31 December, SWCC_{avg} returned to around $0.26 \text{ m}^3 \text{ m}^{-3}$, closing the annual cycle. This corresponds to an overall amplitude of $0.16 \text{ m}^3 \text{ m}^{-3}$, with a recharge duration of about 31 days. The late-season rise in SWCC occurs near the end of the rainy season, as a delayed but rapid response of the groundwater to rainfall, coinciding with the budburst of *Faidherbia albida* in mid-October (Roupsard et al., 2022).

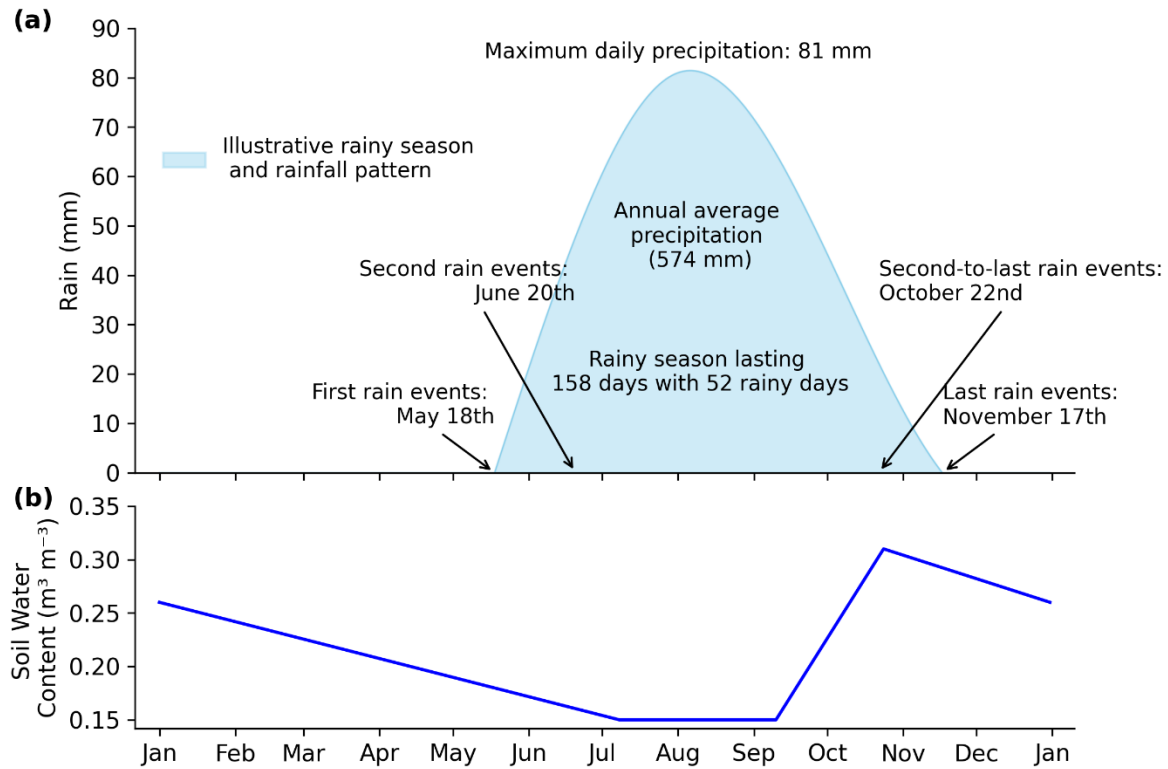


Figure S3: Characteristics of average (a) daily precipitation time series for 2018-2022 and (b) the soil water content in the capillary fringe of the groundwater (SWCC) time series collected for 2019-2021 used for the sensitivity analysis of water availability. All the variables were averaged between years.

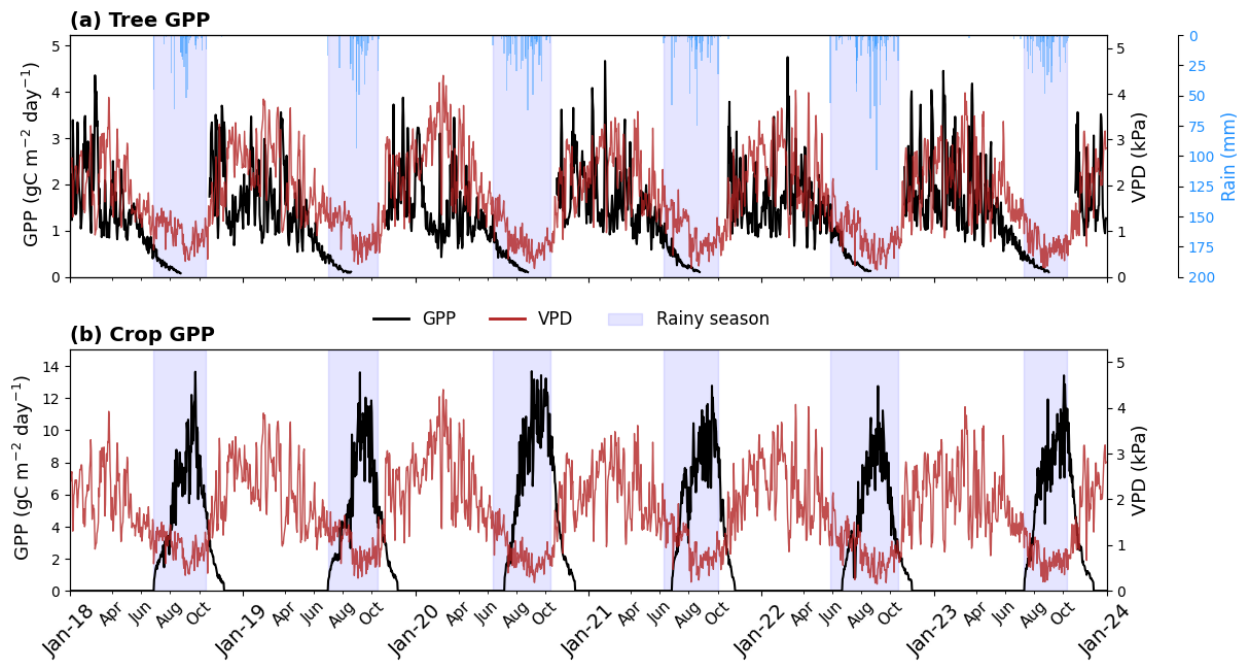


Figure S4: Daily time series comparing simulated gross primary productivity (GPP) (a: tree, b: crop) with vapor deficit pressure (VPD).

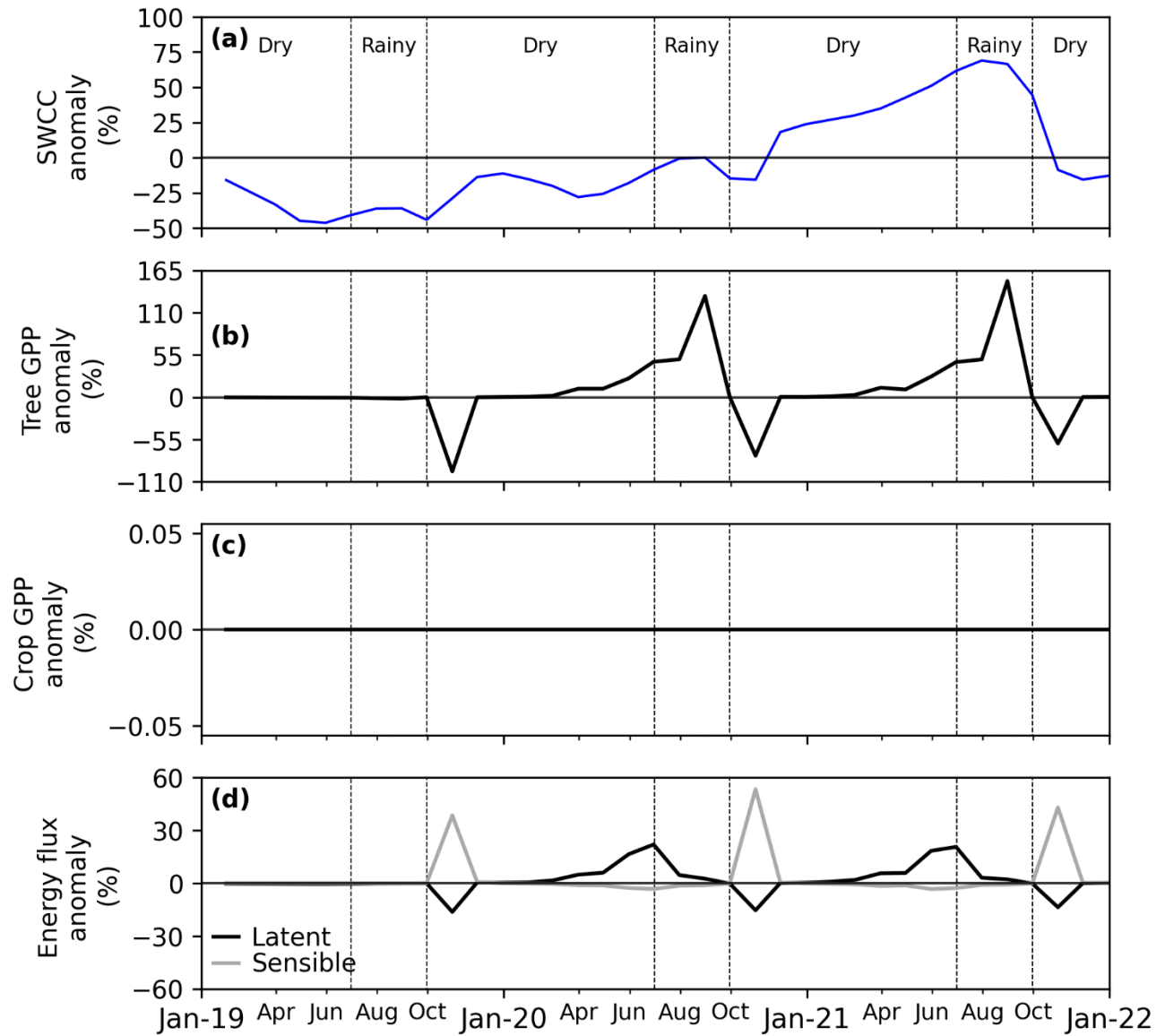


Figure S5: Sensitivity study of monthly anomalies in $R_{avg}SWCC_{var}$ scenario (a) soil water content in the capillary fringe of the groundwater table (SWCC), (b) tree gross primary productivity (GPP), (c) crop GPP, (d) latent and sensible flux. $R_{avg}SWCC_{var}$ is a simulation with average rain and variable SWCC, thus affecting the tree and the ecosystem, but not the crop. The sensitivity is quantified as the anomaly of the $R_{avg}SWCC_{var}$ scenario with respect to $R_{avg}SWCC_{avg}$ (simulation with average rain and average SWCC), considered as the reference scenario.

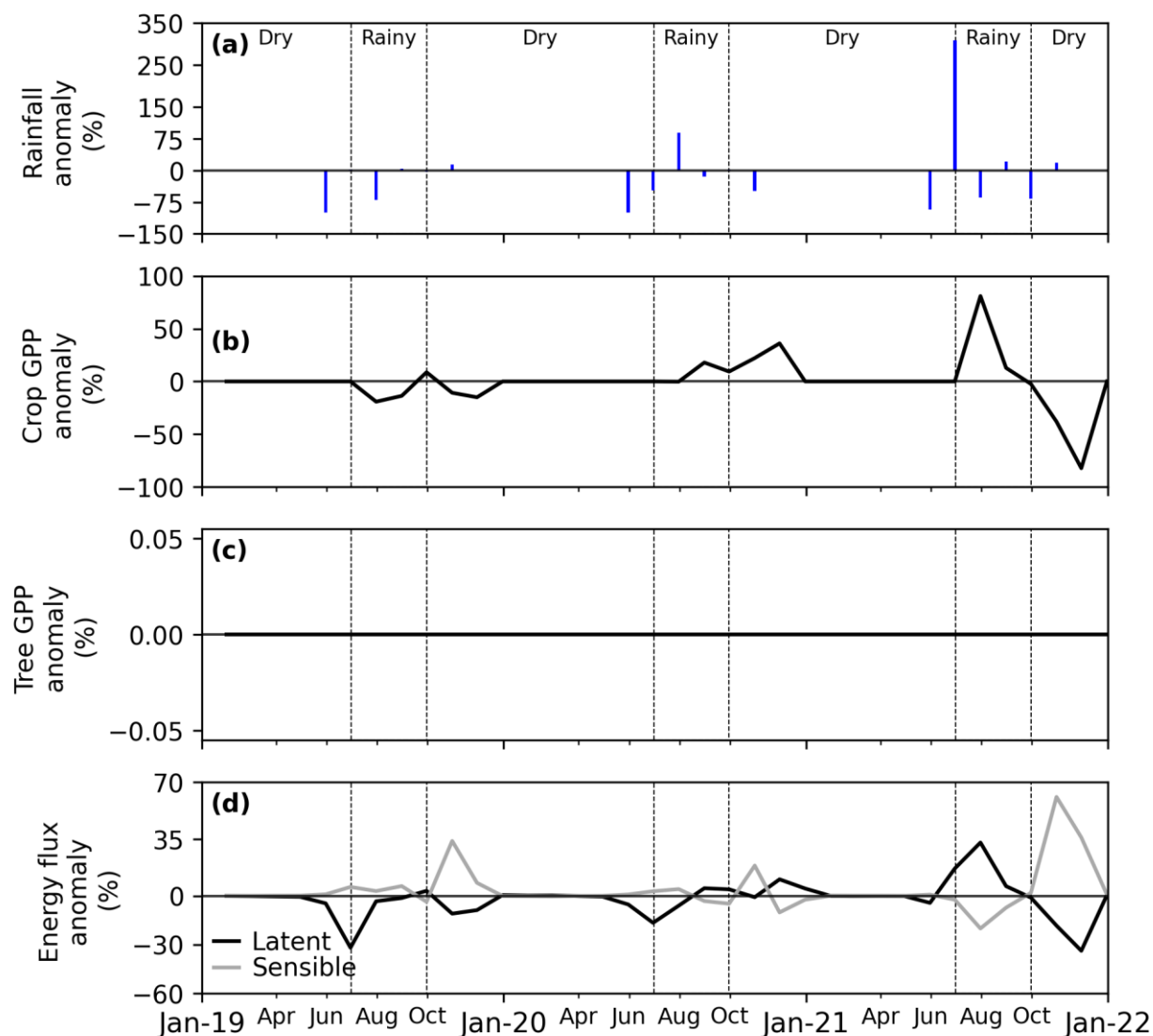


Figure S6: Monthly sensitivity study of anomalies in RvarSWCCavg scenario (a) rainfall, (b) crop gross primary productivity (GPP), (c) tree GPP, (d) latent and sensible flux. RvarSWCCavg is a simulation with variable rain and average SWCC, thus affecting the crop and the ecosystem, but not the tree. The sensitivity is quantified as the anomaly of the RvarSWCCavg scenario with respect to RavgSWCCavg (simulation with average rain and average SWCC), considered as the reference scenario.

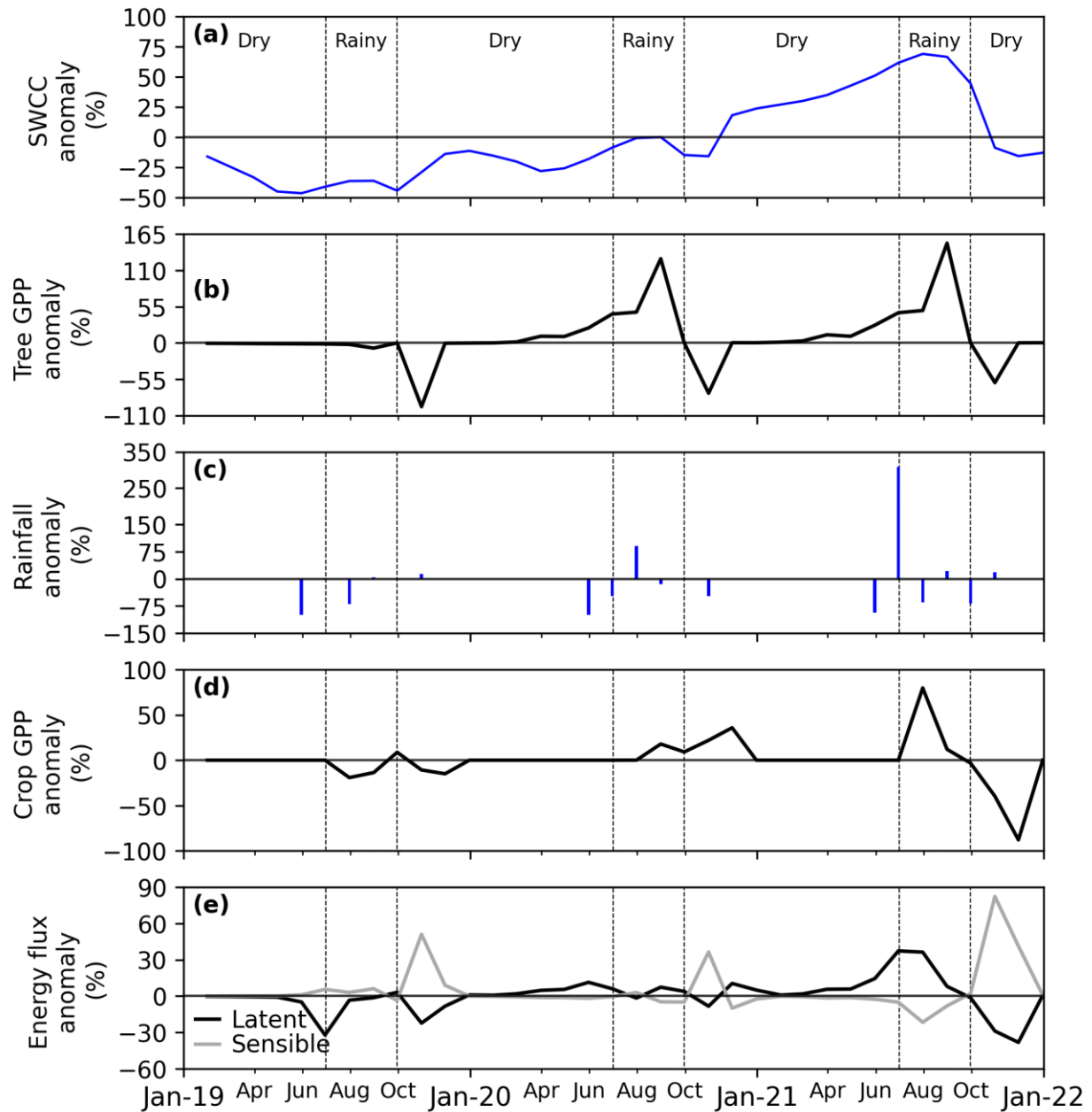


Figure S7: Monthly sensitivity study of anomalies in RvarSWCCvar scenario (a) soil water content in the capillary fringe of the groundwater table (SWCC), (b) tree gross primary productivity (GPP), (c) rainfall, (d) crop GPP, (e) latent and sensible flux. RvarSWCCvar is a simulation with variable rain and variable SWC, where crop, tree, and ecosystem are affected. The sensitivity is quantified as the anomaly of the RvarSWCCvar scenario with respect to RavgSWCCavg (simulation with average rain and average SWCC), considered as the reference scenario.

References

- 230 Bernacchi, C. J., Portis, A. R., Nakano, H., Caemmerer, S. von, and Long, S. P.: Temperature Response of Mesophyll Conductance. Implications for the Determination of Rubisco Enzyme Kinetics and for Limitations to Photosynthesis in Vivo, *Plant Physiol.*, 130, 1992, <https://doi.org/10.1104/pp.008250>, 2002.
- Chen, Q., Baldocchi, D., Gong, P., and Dawson, T.: Modeling radiation and photosynthesis of a heterogeneous savanna woodland landscape with a hierarchy of model complexities, *Agric. For. Meteorol.*, 148, 1005–1020, <https://doi.org/10.1016/j.agrformet.2008.01.020>, 2008.
- 235 Diongue, D. M. L., Roupsard, O., Do, F. C., Stumpp, C., Orange, D., Sow, S., Jourdan, C., and Faye, S.: Evaluation of parameterisation approaches for estimating soil hydraulic parameters with HYDRUS-1D in the groundnut basin of Senegal, *Hydrol. Sci. J.*, 67, 2327–2343, <https://doi.org/10.1080/02626667.2022.2142474>, 2022.
- 240 Diongue, D. M. L., Stumpp, C., Roupsard, O., Orange, D., Do, F. C., and Faye, S.: Estimating water fluxes in the critical zone using water stable isotope approaches in the Groundnut and Ferlo basins of Senegal, *Hydrol. Process.*, 37, e14787, <https://doi.org/10.1002/hyp.14787>, 2023.
- Harley, P. C., Thomas, R. B., Reynolds, J. F., and Strain, B. R.: Modelling photosynthesis of cotton grown in elevated CO₂, *Plant Cell Environ.*, 15, 271–282, <https://doi.org/10.1111/j.1365-3040.1992.tb00974.x>, 1992.
- 245 Kattge, J., Knorr, W., Raddatz, T., and Wirth, C.: Quantifying photosynthetic capacity and its relationship to leaf nitrogen content for global-scale terrestrial biosphere models, *Glob. Change Biol.*, 15, 976–991, <https://doi.org/10.1111/j.1365-2486.2008.01744.x>, 2009.
- Massad, R.-S., Tuzet, A., and Bethenod, O.: The effect of temperature on C₄-type leaf photosynthesis parameters, *Plant Cell Environ.*, 30, 1191–1204, <https://doi.org/10.1111/j.1365-3040.2007.01691.x>, 2007.
- 250 Roupsard, O., Audebert, A., Ndour, A. P., Clermont-Dauphin, C., Agbohessou, Y., Sanou, J., Koala, J., Faye, E., Sambakhe, D., Jourdan, C., le Maire, G., Tall, L., Sanogo, D., Seghieri, J., Cournac, L., and Leroux, L.: How far does the tree affect the crop in agroforestry? New spatial analysis methods in a *Faidherbia* parkland, *Agric. Ecosyst. Environ.*, 296, <https://doi.org/10.1016/j.agee.2020.106928>, 2020.
- Roupsard, O., Faye, W., Sow, S., Diongue, D. M. L., Orange, D., Do, F. C., Jourdan, C., Stumpp, C., and Faye, S.: Inverted phenology of *Faidherbia albida* paced with the dynamics of the water table, *Congrès mondial d'agroforesterie*, public, 5, 1 p., 2022.
- 255 Siegwart, L., Bertrand, I., Roupsard, O., and Jourdan, C.: Contribution of tree and crop roots to soil carbon stocks in a Sub-Saharan agroforestry parkland in Senegal, *Agric. Ecosyst. Environ.*, 352, 108524, <https://doi.org/10.1016/j.agee.2023.108524>, 2023.
- 260 Sow, S., Senghor, Y., Sadio, K., Vezy, R., Roupsard, O., Affholder, F., N'dienor, M., Clermont-Dauphin, C., Gaglo, E. K., Ba, S., Tounkara, A., Balde, A. B., Agbohessou, Y., Seghieri, J., Sall, S. N., Couedel, A., Leroux, L., Jourdan, C., Diaite, D. S., and Falconnier, G. N.: Calibrating the STICS soil-crop model to explore the impact of agroforestry parklands on millet growth, *Field Crops Res.*, 306, 109206, <https://doi.org/10.1016/j.fcr.2023.109206>, 2024.
- Thornley, J. H. M.: Instantaneous Canopy Photosynthesis: Analytical Expressions for Sun and Shade Leaves Based on Exponential Light Decay Down the Canopy and an Acclimated Non-rectangular Hyperbola for Leaf Photosynthesis, *Ann. Bot.*, 89, 451–458, <https://doi.org/10.1093/aob/mcf071>, 2002.
- 265 Von Caemmerer, S.: *Biochemical Models of Leaf Photosynthesis*, Csiro Publishing, 186 pp., 2000.
- Wickens, G. E.: *Role of Acacia Species in the Rural Economy of Dry Africa and the Near East*, Food & Agriculture Org., 144 pp., 1995.